

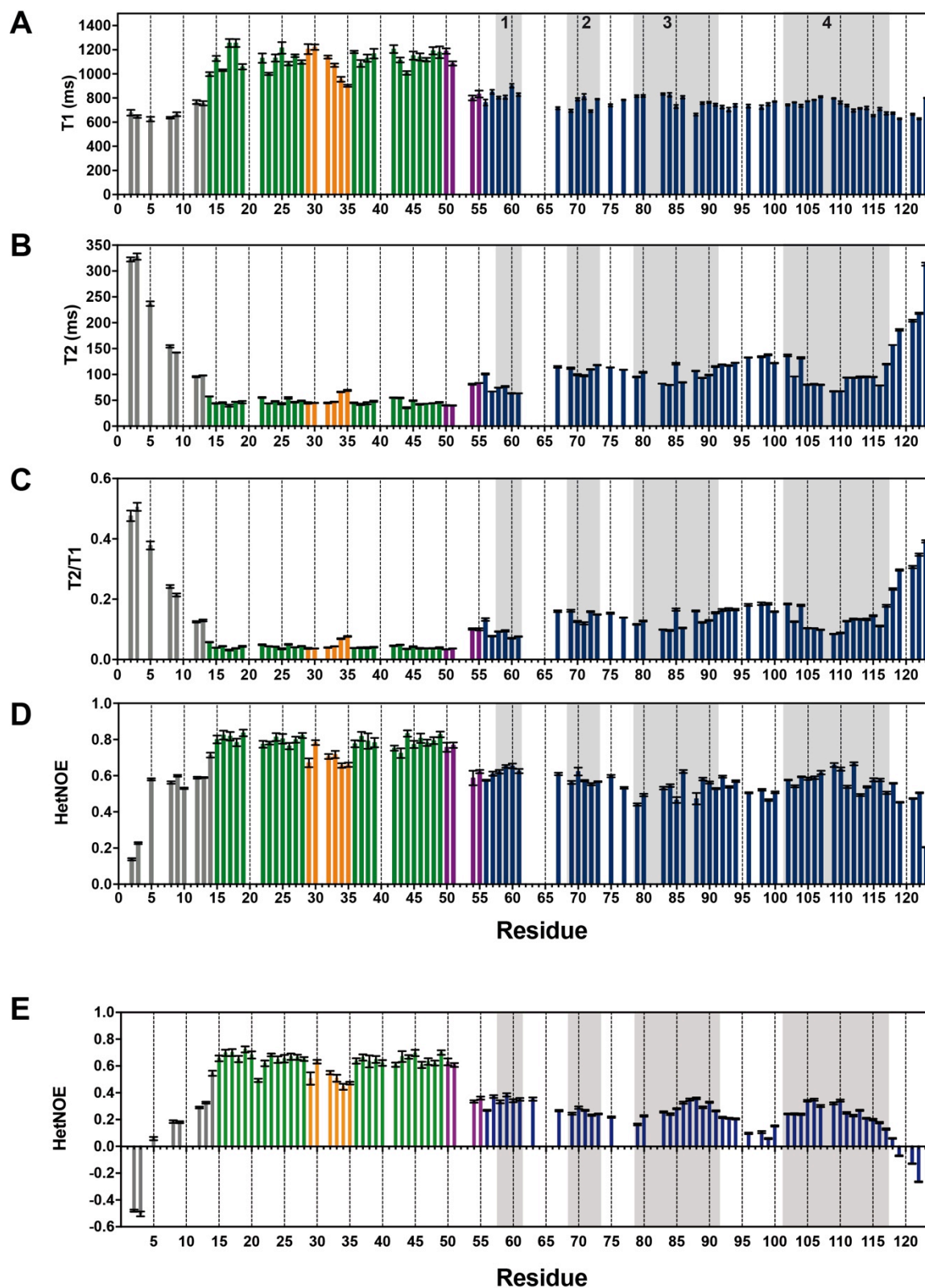
## Supplementary data

### **Modulation of the HIV-1 nucleocapsid dynamics finely tunes its RNA-binding properties during virion genesis**

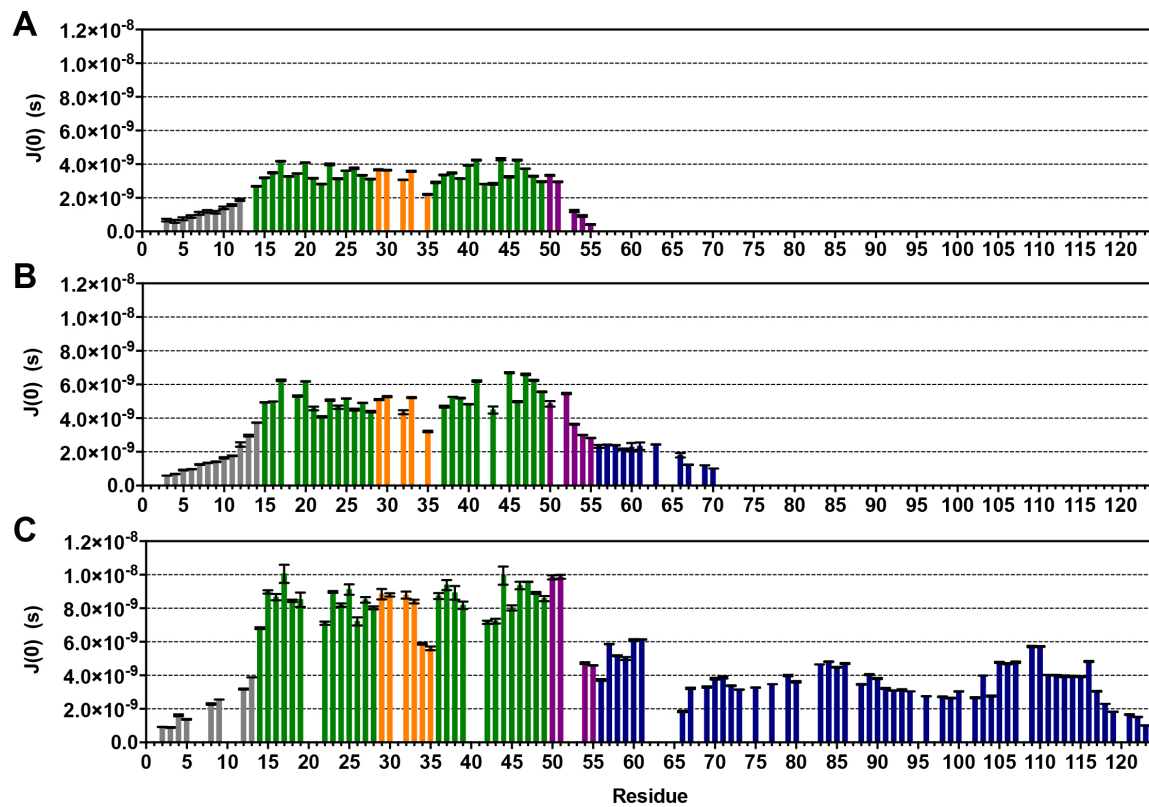
Assia Mouhand<sup>1,2§</sup>, Anissa Belfetmi<sup>3§</sup>, Marjorie Catala<sup>1,2</sup>, Valéry Larue<sup>1</sup>, Loussiné Zargarian<sup>3</sup>, Franck Brachet<sup>1</sup>, Robert J. Gorelick<sup>4</sup>, Carine Van Heijenoort<sup>5</sup>, Gilles Mirambeau<sup>6</sup>, Pierre Barraud<sup>1,2</sup>, Olivier Mauffret<sup>3</sup> & Carine Tisné<sup>1,2\*</sup>



**Supplementary Figure S2.** Dynamic characterization of NCp15 from  $^{15}\text{N}$  NMR relaxation data recorded at 950 MHz (**A**) T1, (**B**) T2, (**C**) T2/T1, (**D**)  $^1\text{H}$ - $^{15}\text{N}$  HetNOE measured at 950 MHz and (**E**)  $^1\text{H}$ - $^{15}\text{N}$  HetNOE measured at 600 MHz. The color code for residues is described on figure 1. The boxes in grey indicated the four regions of p1-p6 domains showing significant secondary structure propensities.

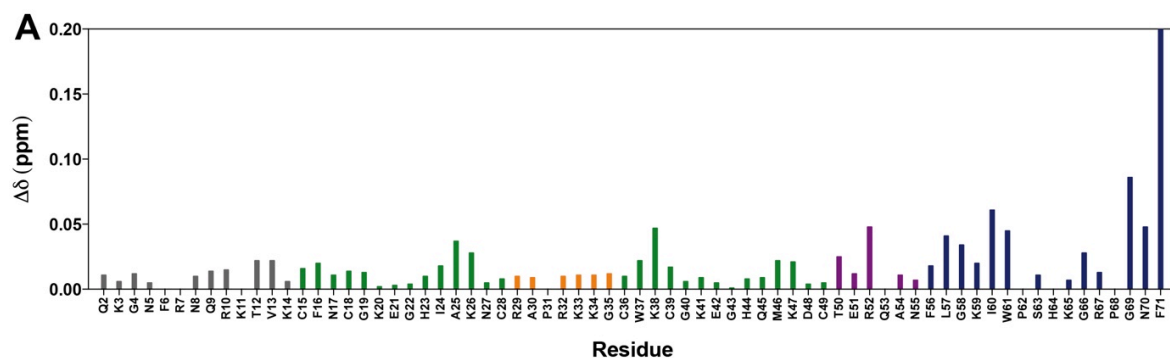


**Supplementary Figure S3.** Spectral densities  $J(0)$  extracted by spectral density mapping from  $^{15}\text{N}$  relaxation data (T1, T2, HetNOE) of (A) NCp7, (B) NCp9 and (C) NCp15 at 950 MHz. The color code for residues is described on figure 1.

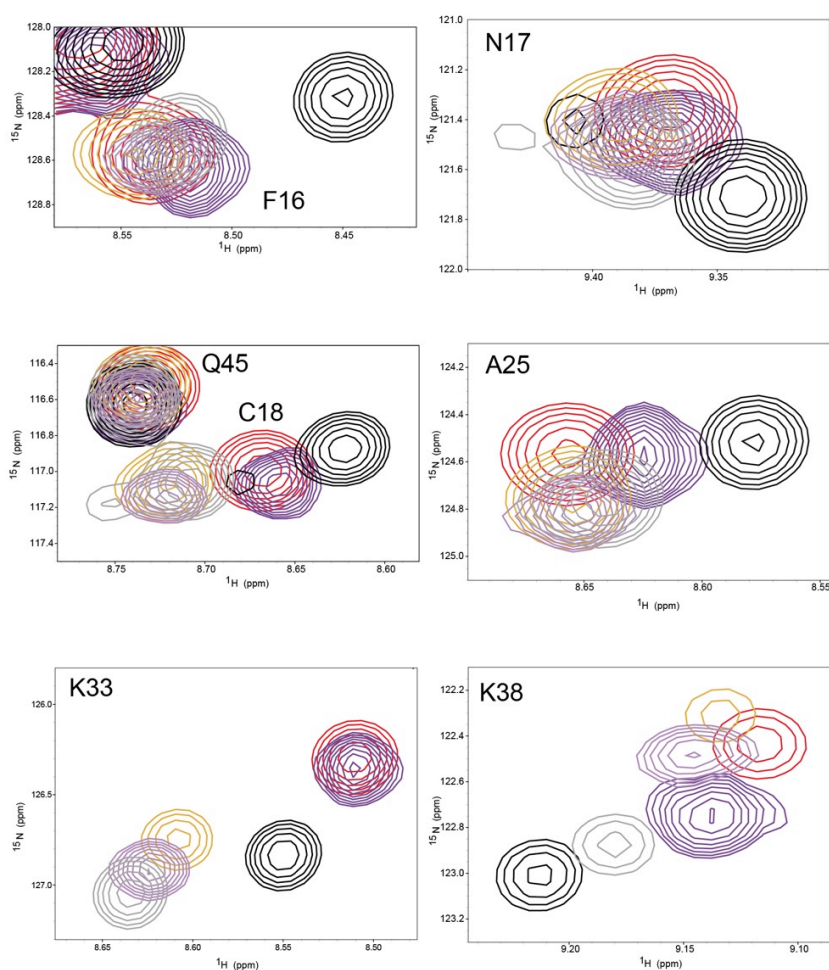


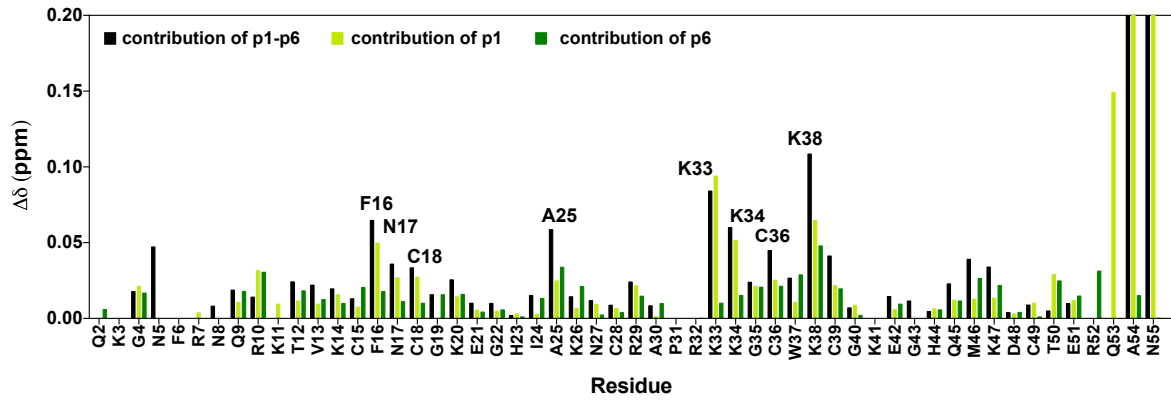
**Supplementary Figure S4.** Analysis of NMR data recorded on nucleocapsid proteins.

**(A)** Contributions of p6 to NCd-p1 chemical shift perturbations measured on the amide groups. The p6 contribution was calculated as the difference in chemical shifts of NCd-p1 amide groups (combined  $^1\text{H}/^{15}\text{N}$  shifts) between NCp15 and NCp9. The color code for residues is described on figure 1. **(B)** Comparison of NMR data recorded on nucleocapsid proteins recorded at 700 MHz at two salt concentrations (25 mM and 500 mM NaCl). Zooms showing amide group resonances of F16, N17, C18, A25, K33 and K38 of NCp7 (Black and grey), NCp9 (purple and light purple), NCp15 (red and orange). **(C)** Contributions of p1-p6 (black bars), p1(light green bars) and p6 (dark green bars) to NCd chemical shift perturbations measured for the amide groups recorded at pH 6.5, 35°C, 700 MHz.

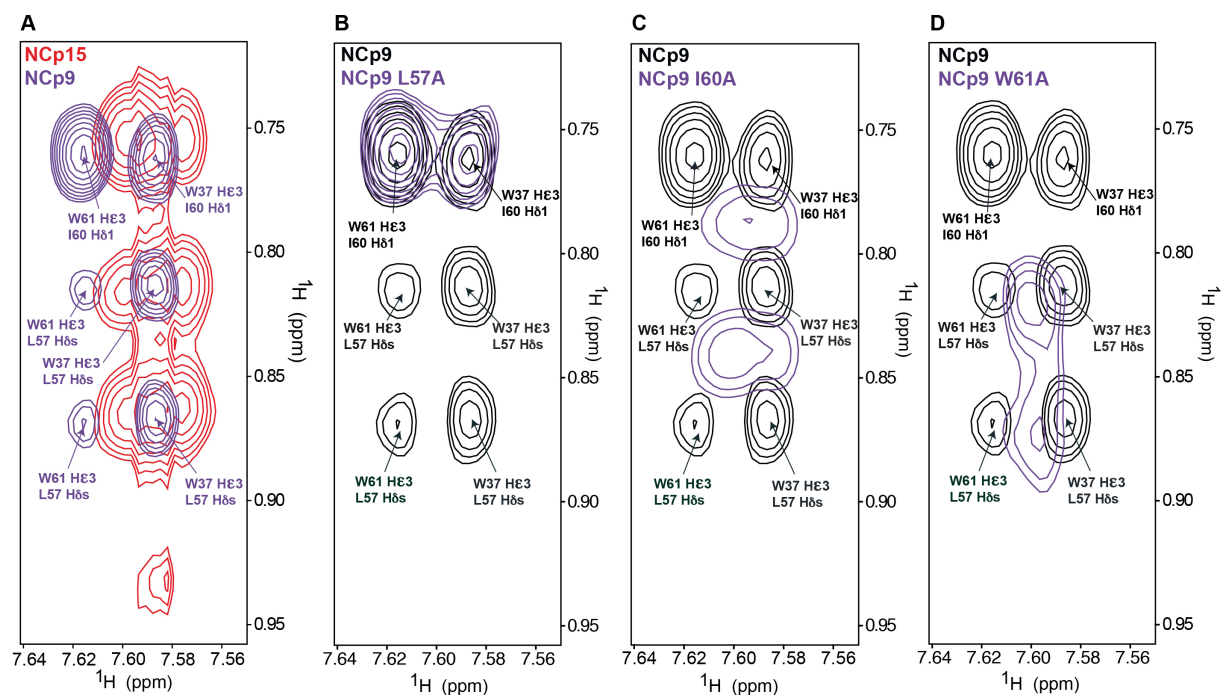


**B** NCp7 (25 mM, 500 mM NaCl) NCp9 (25 mM, 500 mM NaCl) NCp15 (25 mM, 500 mM NaCl)

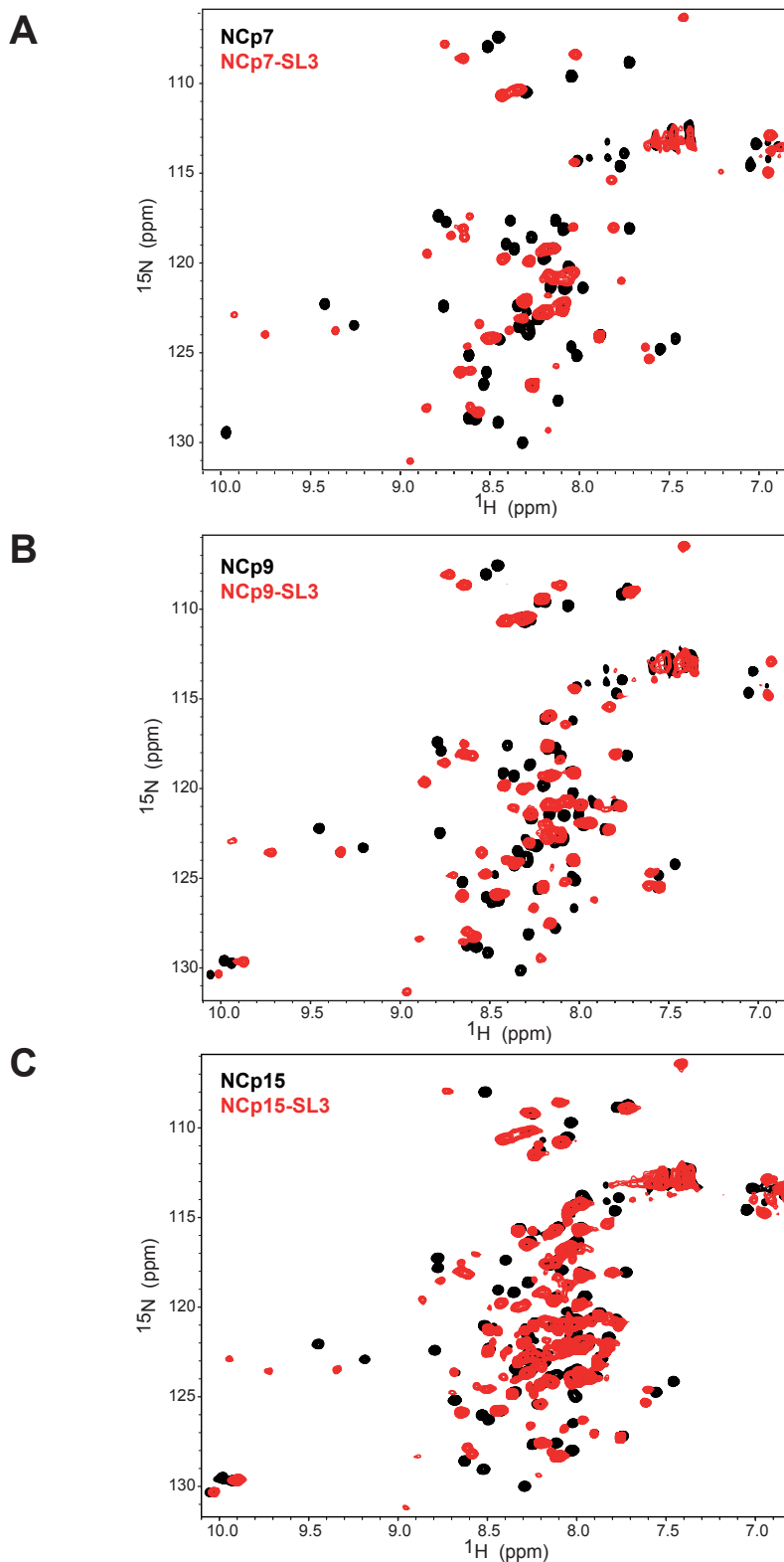


**C**

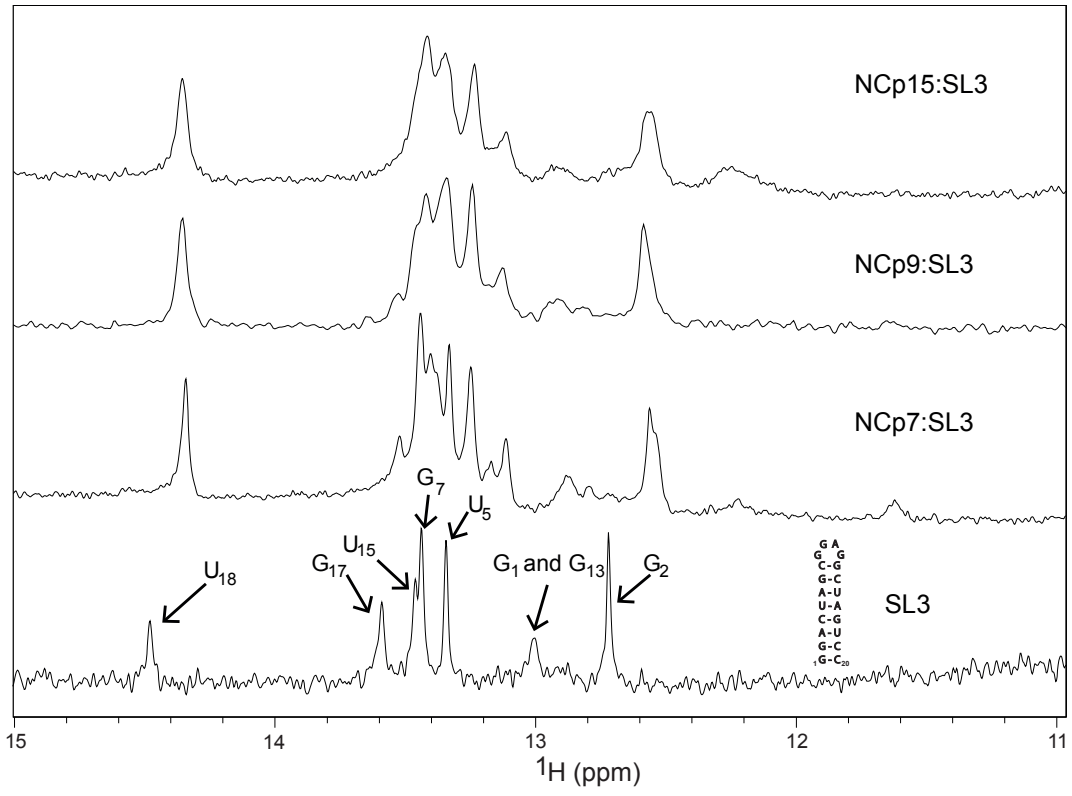
**Supplementary Figure S5.** Analysis of transient interactions through observation of weak NOEs in 2D NOESY recorded in D<sub>2</sub>O. (A) Superposition of 2D NOESY experiments (150 ms, 950 MHz) for NCp15 (in red) and NCp9 (in purple) showing the NOEs between W37 H $\epsilon$ 3 and methyl groups of L57 and I60 ; NOESY experiments (300 ms, 700 MHz) for (B) NCp9 L57A, (C) NCp9 I60A and (D) NCp9 W61A enabling us to unambiguously assign the weak NOEs observed between residues from p1 and NCd described in Figure 2C.



**Supplementary Figure S6.** NMR chemical shift mappings of SL3 binding to the Ncd as a function of its maturation state. Superimposition of  $^1\text{H}$ - $^{15}\text{N}$  BEST-TROSY NMR experiments recorded at 950 MHz for the protein alone (in black) and bound to SL3 (in red) at 1 :1 ratio **(A)** NCp7, **(B)** NCp9 and **(C)** NCp15, **(D)** 1D  $^1\text{H}$  NMR spectra showing imino protons of SL3 alone and in complex with the three forms of the Ncd recorded at 600 MHz and 25°C. The folding of SL3 is the same in the three complexes.

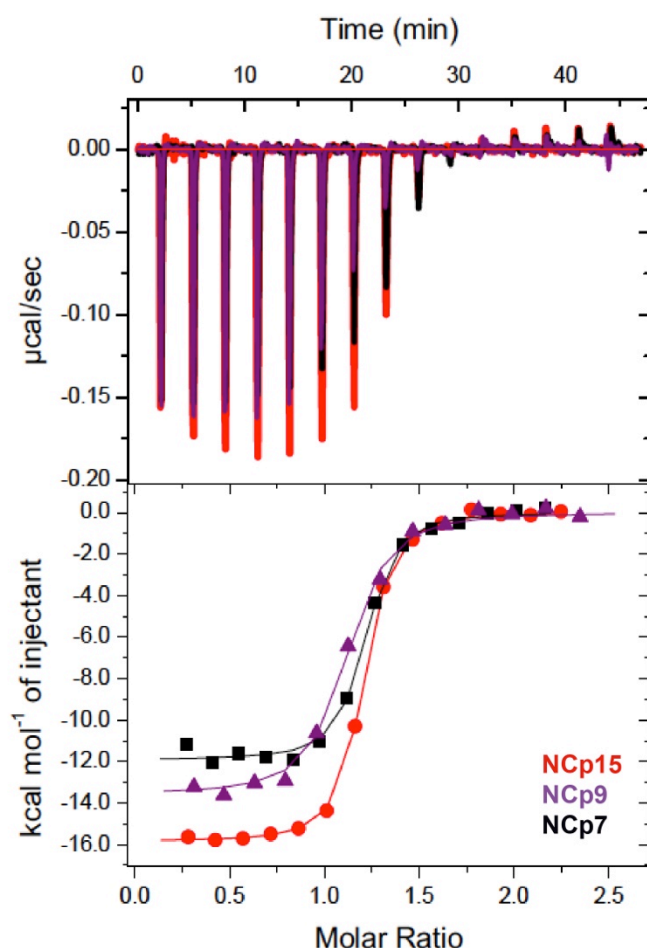


D



**Supplementary Figure S7. (A)** Representative ITC binding isotherms of the calorimetric titration of SL3 by the nucleocapsid proteins, NCp7 (in black), NCp9 (in purple) and NCp15 (in red). **(A)** Raw data with the integration baseline. On the bottom: Data after peak integration and subtraction of blank titration. The line represents the fit to a 1:1 binding model. **(B)** Values of stoichiometry (N) and dissociation constants ( $K_d$ ) extracted from the ITC isotherms.

**A**



**B**

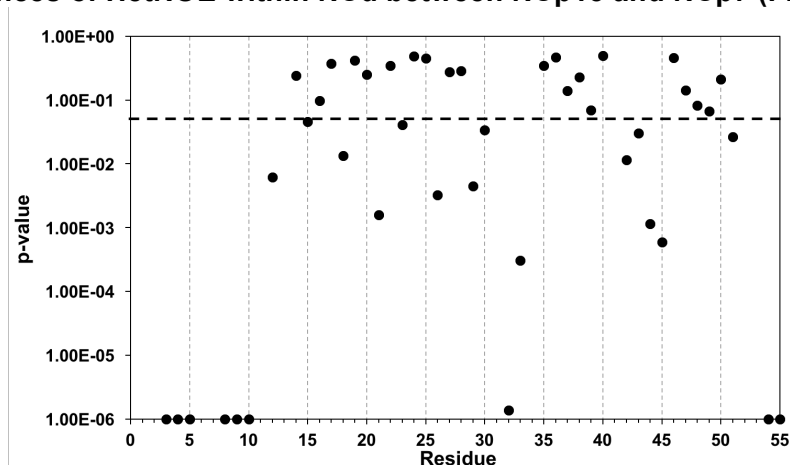
	N	$K_d$ (nM)
NCp7/SL3	$1.16 \pm 0.06$	$24 \pm 4$
NCp9/SL3	$1.06 \pm 0.07$	$44 \pm 4$
NCp15/SL3	$1.14 \pm 0.05$	$20 \pm 1$

Values are reported as means  $\pm$  standard errors. The uncertainties on the fitted parameters were estimated from the data spread and from the uncertainty of the protein concentration determination (5%) (2).

**Supplementary Figure S8.** Statistical analysis of the NMR and ITC data obtained for the three proteins NCp7, NCp9 and NCp15. p-values were calculated using R (<http://www.R-project.org/>) scripts considering that the data follow a normal distribution with a mean value  $\mu$  of 0 and a standard deviation  $\sigma$  that depends on the standard deviations of the data that are compared. We used a p-value inferior to 0.05 to detect significance. This value is indicated as a dotted line in each graph. p-value superior to 0.05 means that the differences of data that are tested are not significantly different from 0 whereas p-value inferior to 0.05 indicate that these differences are significantly different from 0. **(A)** Statistical analysis of the NMR data presented in Figure 1F, for a residue  $i$ , the  $\sigma_i$  value was calculated as  $\sigma_i = \sqrt{(\sigma_{iNCp15})^2 + (\sigma_{iNCp7})^2}$ ,  $\sigma_{iNCp15}$  (respectively  $\sigma_{iNCp7}$ ) being the standard deviation calculated for the measurement of the HetNOE of residue  $i$  in NCp15 (respectively NCp7). p-values smaller than 1E-06 have been set to 1E-06 to permit their visualization **(B)** Statistical analysis of the NMR data presented in Figure 2B using a  $\sigma$  value of 0.02 ppm, **(C)** Statistical analysis of the NMR data presented in Figure 3A and 3B using a  $\sigma$  value of 0.03 ppm to take into account that the NMR spectra of the complexes are less resolved, **(D)** p-values calculated for the ITC data presented in Figure 3C using the standard errors estimated for each thermodynamic function as defined in Materials and Methods.

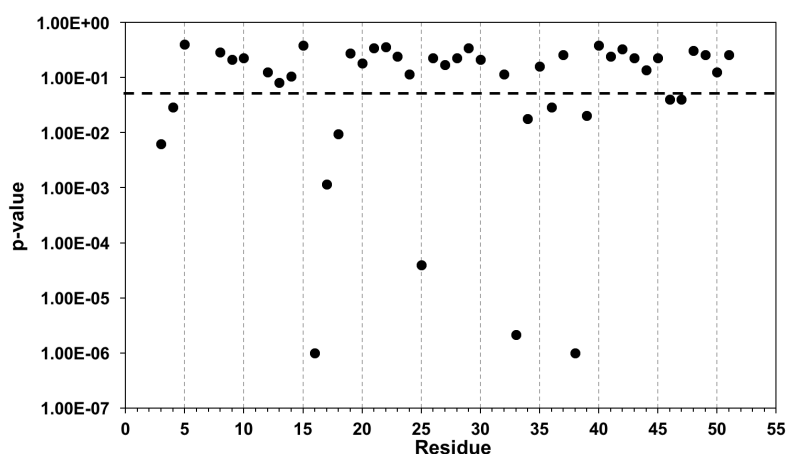
**A**

**Differences of HetNOE within NCd between NCp15 and NCp7 (Figure 1F)**

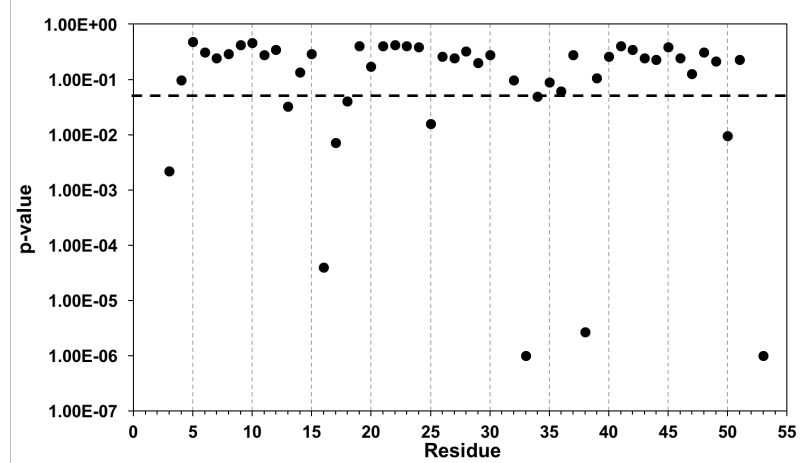


**B**

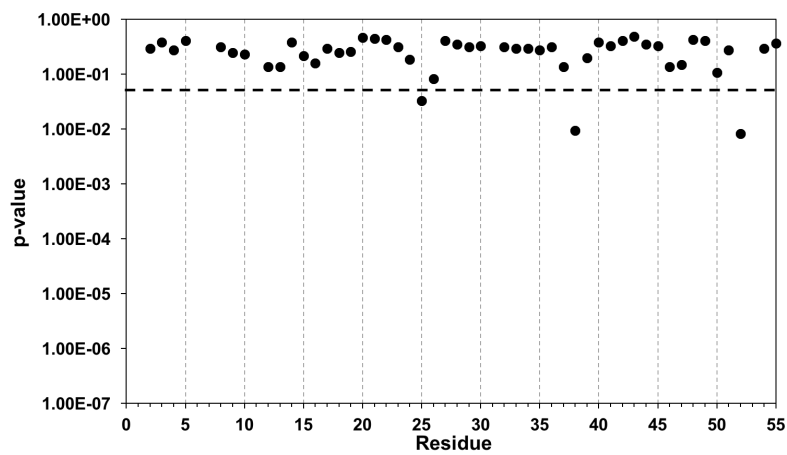
**Chemical shift differences between NCp15 and NCp7 (Figure 2B)**



Chemical shift differences between NCp9 and NCp7 (Figure 2B)

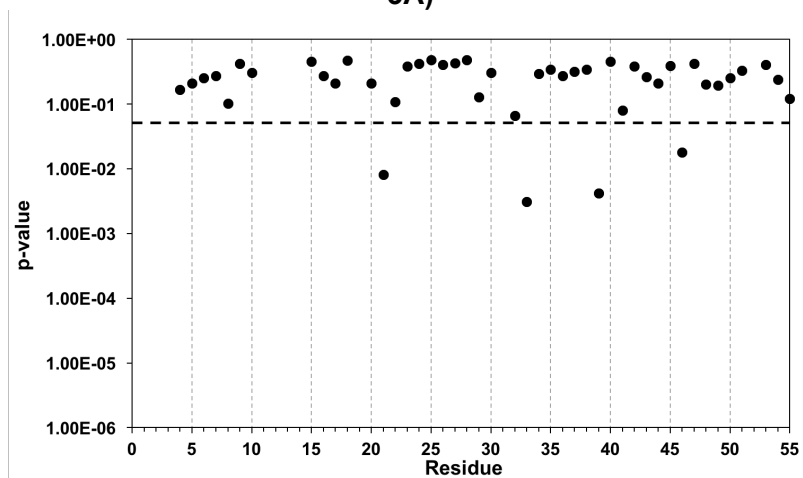


Chemical shift differences between NCp15 and NCp9 (Figure 2B)

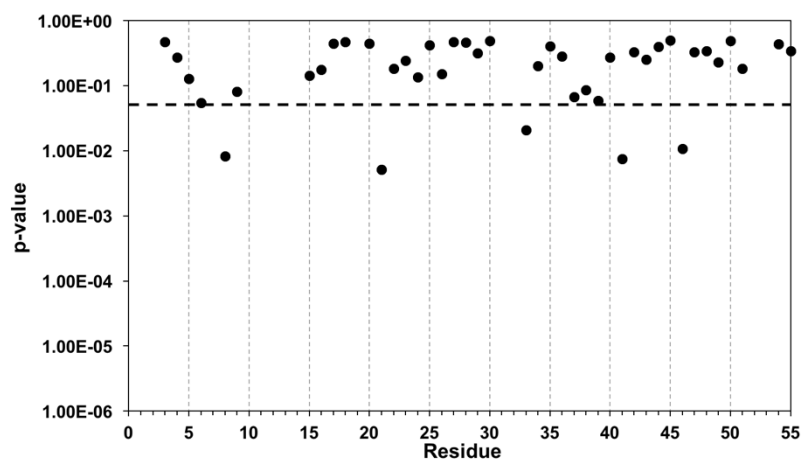


C

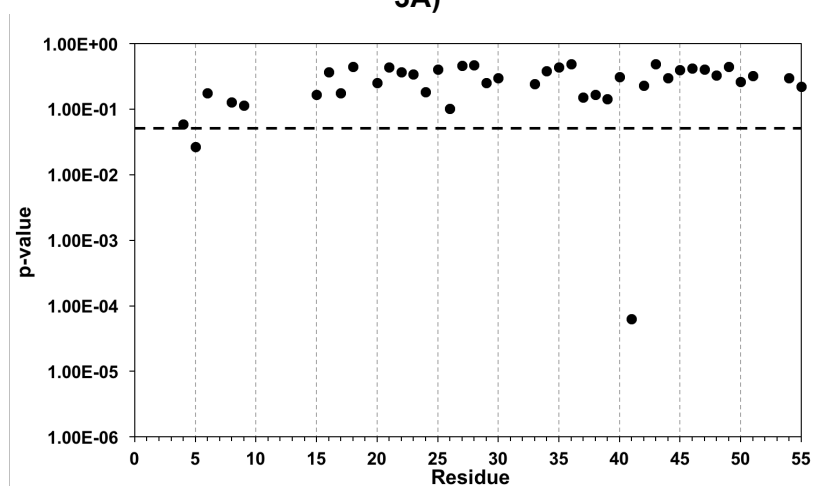
Chemical shift differences between NCp7/SL3 and NCp9/SL3 within the NCd (Figure 3A)



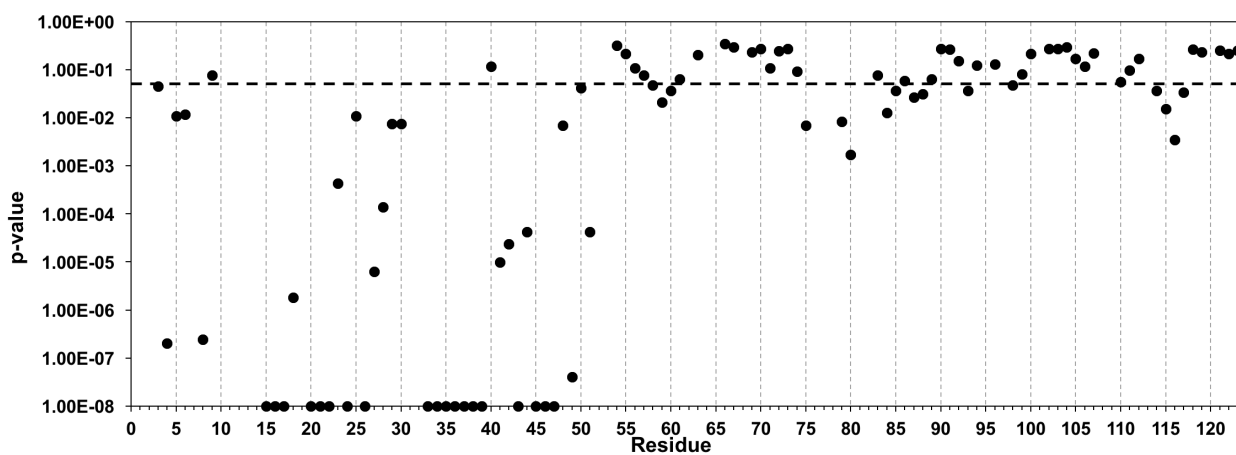
Chemical shift differences between NCp7/SL3 and NCp15/SL3 within the NCd (Figure 3A)



Chemical shift differences between NCp15/SL3 and NCp9/SL3 within the NCd (Figure 3A)



Chemical shift differences between NCp15 and NCp15/SL3 (Figure 3B)



## D

$\Delta G$ (kcal/mol)	NCp7/SL3	NCp9/SL3	NCp15/SL3
NCp7/SL3		1.00E-04	0.26
NCp9/SL3			5.5E-13
NCp15/SL3			
$\Delta H$ (kcal/mol)	NCp7/SL3	NCp9/SL3	NCp15/SL3
NCp7/SL3		0.07	1.00E-08
NCp9/SL3			2.00E-03
NCp15/SL3			
$-\Delta S$ (kcal/mol)	NCp7/SL3	NCp9/SL3	NCp15/SL3
NCp7/SL3		0.02	5.3E-08
NCp9/SL3			0.02
NCp15/SL3			

1. Solyom, Z., Schwarten, M., Geist, L., Konrat, R., Willbold, D. and Brutscher, B. (2013) BEST-TROSY experiments for time-efficient sequential resonance assignment of large disordered proteins. *J Biomol NMR*, **55**, 311-321.
2. Tellinghuisen, J. and Chodera, J.D. (2011) Systematic errors in isothermal titration calorimetry: concentrations and baselines. *Anal Biochem*, **414**, 297-299.